



## Preparation, Characterization of Mg and Al Co-doped ZnO nanoparticles and Its Application in Congo Red Dye Remediation



S. Arul<sup>1\*</sup> and T. Senthilnathan<sup>2</sup>

<sup>1</sup>Department of Physics, GRT Institute of Engineering and Technology, Tiruttani, Thiruvallur Dt.-631209, (Tamilnadu) India

<sup>2</sup>Department of Physics, Vellammal Engineering College, Ambattur-Red Hills Road,

A simple co-precipitation method at normal temperature was used to prepare Mg and Al co-doped ZnO nanoparticles. The structure and chemical properties of synthesized nanoparticles were characterized by various techniques such as XRD, FTIR, SEM-EDX, UV-Visible Spectroscopy and AFM, whereas the photo-catalysis study of congo red (CR) was performed by UV/VIS spectrophotometry. The XRD results exhibited that Mg, Al co-doped ZnO nanoparticles possess hexagonal wurtzite structure. The SEM analysis suggested varying nano morphology of synthesized nanoparticles and the purity of the sample was checked by EDX analysis. Mg, Al co-doped ZnO nanoparticles were subjected for the photo-degradation of congored dye (CR) in aqueous medium under UV-light irradiation. The photo-degradation study revealed that the Mg, Al co-doped ZnO nanoparticles is a promising substance for the hazardous ecological remediation.

**Keywords:** ZnO nanoparticles, Soft-chemical method, Congored, Photodegradation.

### Introduction

In the past few decades, dyes are significantly used additive or colorant in many industries like textile, leather, paper, printing, ink, pharmaceutical, cosmetics and food industries. The application of synthetic dye over natural dye has been increased in recent years due to its performance and low cost. As per the reports, over 10000 tons of dyes were produced annually which ultimately resulted in increasing public interest about the dyeing waste water treatment<sup>1</sup>. The waste water containing high concentration of dyes is highly toxic to the environment and adds colour to the water that prevents the penetration of sunlight<sup>2</sup>. In addition to this, chemicals also cause carcinogenic and mutagenic effects to the life around it.

The predominant dye Congo red (CR) used by the textile industries is the sodium salt of 3, 3'-([1, 1'-biphenyl]-4, 4'-diyl) bis 4-aminonaphthalene-1-sulfonic acid (C<sub>32</sub>H<sub>22</sub>N<sub>6</sub>Na<sub>2</sub>O<sub>6</sub>S<sub>2</sub>). Inefficient

decolourisation because of fading resistance and persistence to biological degradation was the complication occurred. To overcome these complications, endless development of advanced water treatments has been progressed. Many numbers of studies have been reported in the development of dye removal in water. The major removal methods are physical<sup>3</sup> (Precipitation, adsorption, filtration, flocculation), chemical<sup>4</sup> (Photochemical decolourisation, ozonation, Chlorination) and biological methods<sup>5</sup> (Biological oxidation). About 95% of CR removal by adsorption after 24 hr of contact time was achieved earlier by researchers<sup>6</sup>. Despite the CR removal, adsorption separates dyes from waste water and thus it is not a destructive process. Further, acid functional group in CR dye inhibits them being attached by the low cost adsorbents<sup>7</sup>. Activated carbon is highly effective and that can bind acid dyes like CR but high cost minimizes its usage<sup>8</sup>. All other treatments needed

\*Corresponding author e-mail: [kirthickarul@gmail.com](mailto:kirthickarul@gmail.com)

Received 9/08/2019; Accepted 15/10/2019

DOI: 10.21608/ejchem.2019.15825.1957

©2019 National Information and Documentation Center (NIDOC)

to treat the waste stream resulted in inefficient decolorization. Subsequently, much of attention has been required for the degradation of dyes. Earlier reports suggested that advance oxidation processes showcased high efficiency in dye degradation processes. Equally, photocatalytic degradation has also attracted researchers to treat organic pollutant. Photocatalysis is proficient to treat wide range of organic pollutant at ambient temperature and pressure to degradable product.

Zinc oxide (ZnO) mediated based photodegradation has attracted extensive interest owing to its great advantages in the complete removal of organic pollutants from wastewater. This is mainly because of its various merits such as optical-electronic properties, low-cost, chemical stability and nontoxicity<sup>9</sup>. The main aim of this paper is to produce a condensed and coherent overview on the photocatalytic degradation of azo dyes in the presence of ZnO doped with selective transition metals, which can serve as a ready reference for future scientific endeavors in this area. Photodegradation of azo dyes using transition metal doped ZnO has been found to be very effective for the treatment of dye-contaminated solutions. The basis of the reaction is photoredox process. In this process, an important role is played by molecular oxygen and other active species, such as  $O_2^-$ ,  $H_2O^-$ ,  $H_2O_2$ , and  $\cdot OH$ , which are generated in a sequence of reactions<sup>10</sup>. They make the photocatalytic processes more efficient resulting in enhanced dye degradation via the formation of intermediates such as aromatic amines, phenolic compounds and several organic acids. Although azo dyes are one of the most commonly used class of dyes in industrial applications, limited literature is available on their remediation from effluents using ZnO doped with transition metals.

### **Materials and Methods**

The essential chemicals for the preparation of ZnO nanoparticles by soft chemical method were purchased from Merck and used as a precursors and double distilled water was used as solvent.

#### *Synthesis of Mg and Al Codoped ZnO Nanoparticles*

Zinc nitrate hexahydrate (1M), Magnesium nitrate hexahydrate (0.05 M) and Aluminium nona hydrate (0.05 M) were used as precursors and methods as mentioned in the earlier reports<sup>11</sup>. The salts were dissolved in 100 ml distilled water

in magnetic stirrer for 30 mins. A solution of NaOH (2M) was mixed with starting solution to get a large amount of white precipitate under constant stirring at 45°C. By using distilled water, the precipitates were filtered and washed; then dried in hot air oven at 120°C for 4 hours, and the precipitates were powdered in an agar mortar. The final powder was calcined at 450°C for 3 hours and allowed for cooling in furnace. The nanomaterials were collected for further characterization studies. Mg and Al co-doped ZnO obtained by above-mentioned procedure was collected and assigned as Z, Z<sub>A</sub>, Z<sub>B</sub>, Z<sub>C</sub> and Z<sub>D</sub> (Table 1).

#### *Photodegradation analysis*

About 10 mg/L of congo red dye and 50 ml of distilled water with 40 mg of Mg and Al co-doped ZnO nanomaterials were placed under UV irradiation for the degradation of dye in different time interval (0, 30, 60, 90, 120, 150 and 180 minutes). The influence of UV light sources on photo-degradation of congo red dye was supported with a 30 W mercury lamp and the decomposition effect was measured by UV-absorption measurement.

### **Results and Discussion**

#### *XRD Analysis*

Figure 1. shows the X-ray diffraction pattern of un-doped ZnO in comparison with different concentrations of Mg & Al co-doped ZnO nanoparticles synthesized by soft chemical method at 450°C using X-ray diffractometer (BRUKER, Germany, Model-D8-Advance) with Cu K<sub>α</sub> radiation source ( $\lambda = 1.54060 \text{ \AA}$ ). All diffraction peaks corresponded to hexagonal wurtzite structure of ZnO with (JCPDS No.800075)<sup>12</sup>. The peaks of co-doped ZnO had high intensity compared with un-doped ZnO and diffraction intensity increased with magnesium concentration. The average particle size was calculated by Debye Scherrer's formula<sup>13</sup>,

$$D = \frac{0.9\lambda}{\beta \cos \theta} \quad (1)$$

Where, D is average particle size,

$\lambda$  is incident wavelength of X-ray beam,

$\beta$  - full-width at half-maximum (FWHM) and

$\theta$  is Bragg's diffraction angle respectively.

The calculated particle sizes were 52 nm for un-doped ZnO and 40 nm, 38 nm, 34 nm,

37 nm for samples  $Z_A$ ,  $Z_B$ ,  $Z_C$  and  $Z_D$  of Mg, Al co-doped ZnO nanomaterials respectively. The nanoparticles size of sample  $Z_C$  was decreased when compared with un-doped ZnO and samples  $Z_A$ ,  $Z_B$  &  $Z_D$  of Mg & Al co-doped ZnO.

#### FT- IR spectrum analysis

Figure 2. shows the FTIR spectra of prepared un-doped ZnO and Mg & Al co-doped ZnO ( $Z_A$ ,  $Z_B$ ,  $Z_C$  and  $Z_D$ ) nanoparticles on KBr pellets using SHIMADZU FTIR 8400S, Europe in the range 4000-500  $\text{cm}^{-1}$ . The bands perceived at 481.17  $\text{cm}^{-1}$  for un-doped ZnO, and 480.90  $\text{cm}^{-1}$ , 460.88  $\text{cm}^{-1}$ , 490.90  $\text{cm}^{-1}$  and 470.89  $\text{cm}^{-1}$  for samples  $Z_A$ ,  $Z_B$ ,  $Z_C$  and  $Z_D$  of Mg & Al co-doped ZnO nanoparticles were associated to metal oxide. It was admitted that the peaks range of 410 – 735  $\text{cm}^{-1}$  corresponded to ZnO as reported earlier<sup>14</sup>. Peaks at 1384.26  $\text{cm}^{-1}$  for Un-doped ZnO and samples  $Z_A$ ,  $Z_B$ ,  $Z_C$  and  $Z_D$  were attributed to the bending frequency of oxygen stretching mode<sup>15</sup>. The presence of peak around 3445.12  $\text{cm}^{-1}$  for un-doped ZnO and the band at 3451.07, 3445.73, 3446.32 and 3444.41  $\text{cm}^{-1}$  for  $Z_A$ ,  $Z_B$ ,  $Z_C$  and  $Z_D$  of Mg & Al co-doped ZnO due to O-H stretching vibrations<sup>16</sup>.

#### SEM Analysis

Figure 3. indicates the pictures of Un-doped ZnO ( $Z$ ) and Mg and Al co-doped ZnO ( $Z_B$ ) nanoparticles obtained in JEOL JSM 6390LV, Japan, a high performance, low cost scanning electron microscope with a high resolution of 3.0nm. The SEM images revealed that prepared nanoparticles were non-uniform in size and almost in spherical morphology<sup>17</sup>. The surface agglomeration was large in un-doped ZnO compared to co-doped ZnO<sup>18</sup>. The nanoparticle size of un-doped ZnO and Mg, Al co-doped ZnO nanoparticles were calculated to be around 85 nm (0.085 $\mu\text{m}$ ).

Figure 4. indicates the EDAX spectra attained from EDAX PV 9760 detector for energy dispersive X-ray spectroscopy associated with JEOL JSM 6390LV SEM instrument. of Un-doped ZnO and Mg, Al co-doped ZnO nanoparticles. Fig. 4 (i) shows that the elements of Zn and O were present in un-doped nanomaterials and Fig. 4 (ii) indicates the presence of Mg, Al, in the host lattice and also indicates the absence of impurities it correlates with the XRD analysis<sup>19</sup>. The greater peak in a spectrum indicates that high concentration of element presents in doped and un-doped nanomaterials<sup>20</sup>. In Fig. 4 (i) & (ii) Zn element comparatively exhibited higher peaks with another element such as Mg, Al and O.

#### UV-Visible Spectroscopy

Figure 5. shows the optical absorption spectra of un-doped ZnO and Mg, Al co-doped ZnO ( $Z_A$ ,  $Z_B$ ,  $Z_C$  and  $Z_D$ ) nanoparticles using JASCO (V-530), UV-Vis spectrophotometer, USA in the absorption range of 190-1000nm. The wavelength of prepared nanomaterials optical absorption spectra was 379 nm for un-doped ZnO and 374 nm, 369 nm, 371 nm and 374 nm for  $Z_A$ ,  $Z_B$ ,  $Z_C$  and  $Z_D$  of Mg, Al co-doped ZnO nanoparticles respectively. The absorption peak towards the lower wavelength with a blue shift and compared with un-doped ZnO, the absorption peak of doped nanomaterials towards the longer wavelength with red shift, it was ascribed to the small changes in the particle size with rising Mg and Al concentration. The band gap energy values were calculated using the following equation<sup>21</sup>,

$$E = (hc)/(\lambda) \quad (2)$$

Where h is Planck's constant, c is the velocity of light and  $\lambda$  is the wavelength of light and the obtained values were 3.27eV for un-doped ZnO and 3.32eV, 3.36eV, 3.34eV, 3.32eV for samples  $Z_A$ ,  $Z_B$ ,  $Z_C$  and  $Z_D$  of Mg, Al co-doped ZnO nanoparticles. The difference in absorption was established by the presence of doping agents<sup>22</sup>.

#### AFM Analysis

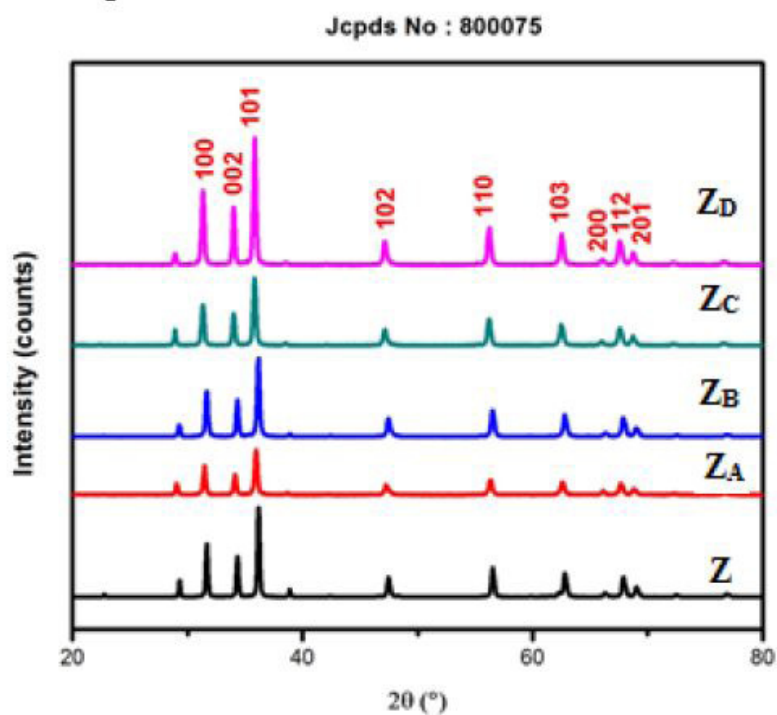
Figure 6. shows the AFM analysis of synthesized Un-doped ZnO ( $Z$ ) and  $Z_B$  nanoparticles by soft chemical method using AFM instrument made in USA (Model-PicoSPM-2100). The average size of the particles was detected as 61 nm for Un-doped ZnO and 37nm for Mg and Al co-doped ZnO which was in good agreement with XRD analysis. The appearance of AFM images with regular shape and random arrangement was observed<sup>23</sup>.

#### Investigation of Photodegradation of Un-doped ZnO and Mg, Al Co-doped ZnO Np'S

Figure 7 exhibits the photodegradation spectra of Un-doped ZnO ( $Z$ ) and  $Z_B$  nanocomposites. The prepared nanoparticles were absorbed by UV light, and electrons were stimulated from the valence band to the conduction band. The light energy caused holes and reacted with water and hydroxyl radical was created. The hydroxyl radical was extremely strong, non-selective oxidant and oxidizing agent which leads to the degradation of organic chemicals. The light energy caused electrons and reacted with molecular oxygen, then superoxide radical anions were generated which was responsible for degradation of dye solution.

TABLE 1. The composition of prepared Nanoparticles.

S.No.	Nanoparticles	Composition
1	Z	Undoped ZnO
2	Z <sub>A</sub>	Mg <sub>0.04</sub> Al <sub>0.01</sub> co-doped ZnO
3	Z <sub>B</sub>	Mg <sub>0.03</sub> Al <sub>0.02</sub> co-doped ZnO
4	Z <sub>C</sub>	Mg <sub>0.02</sub> Al <sub>0.03</sub> co-doped ZnO
5	Z <sub>D</sub>	Mg <sub>0.01</sub> Al <sub>0.04</sub> co-doped ZnO

Fig. 1. XRD patterns of (i) Z (ii) Z<sub>A</sub> (iii) Z<sub>B</sub> (iv) Z<sub>C</sub> and (v) Z<sub>D</sub>

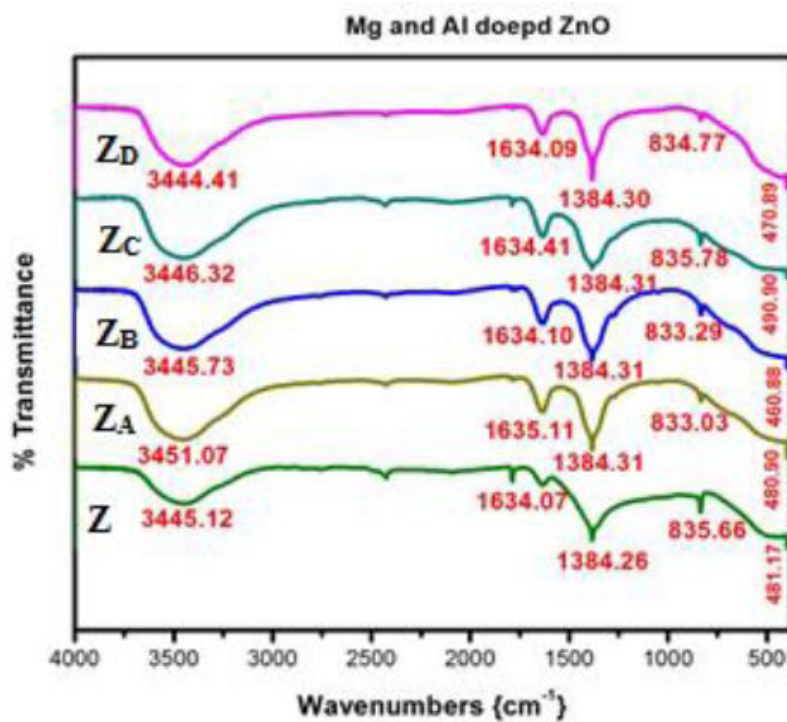


Fig. 2. FT- IR Spectrum of (i) Z and (ii) Z<sub>A</sub> (iii) Z<sub>B</sub> (iv) Z<sub>C</sub> (v) Z<sub>D</sub>

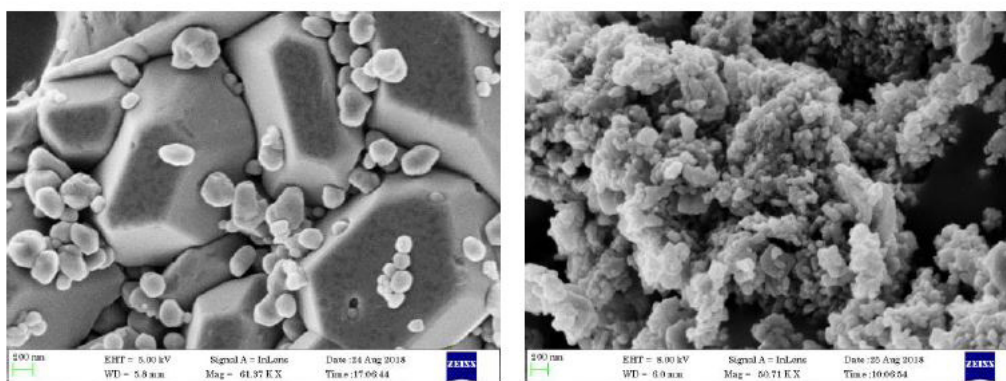


Fig. 3. SEM analysis of (i) Z and (ii) Z<sub>B</sub> 3.4 EDAX Analysis

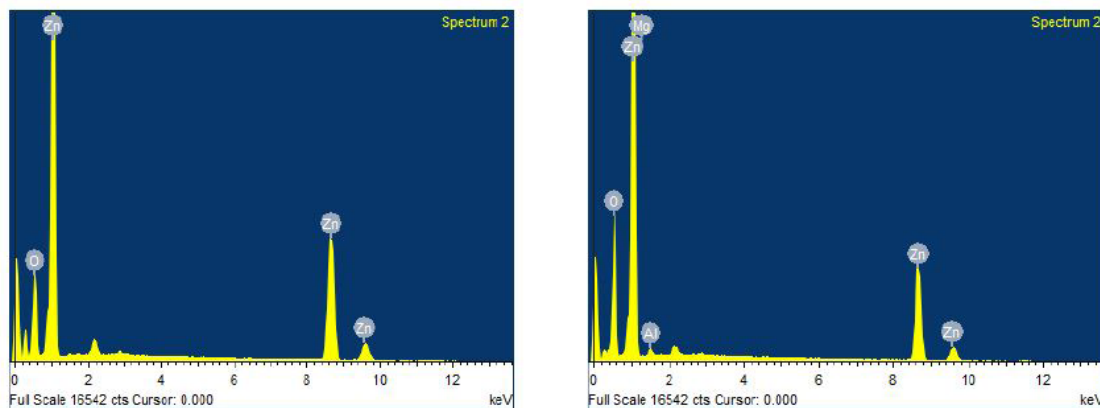


Fig. 4. EDAX analysis of SEM analysis of (i) Z and (ii)  $Z_B$

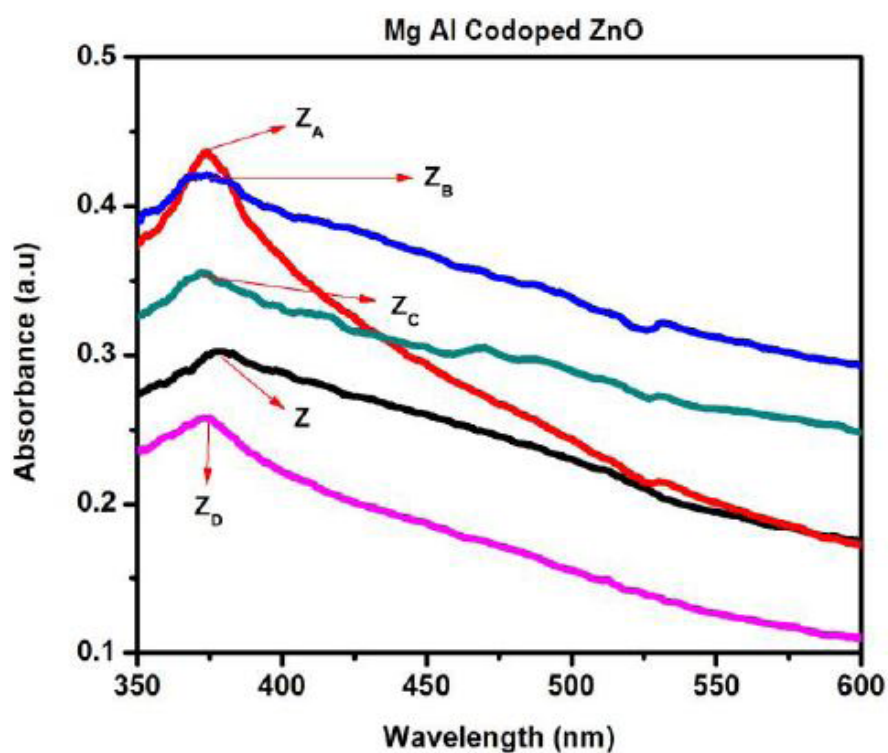
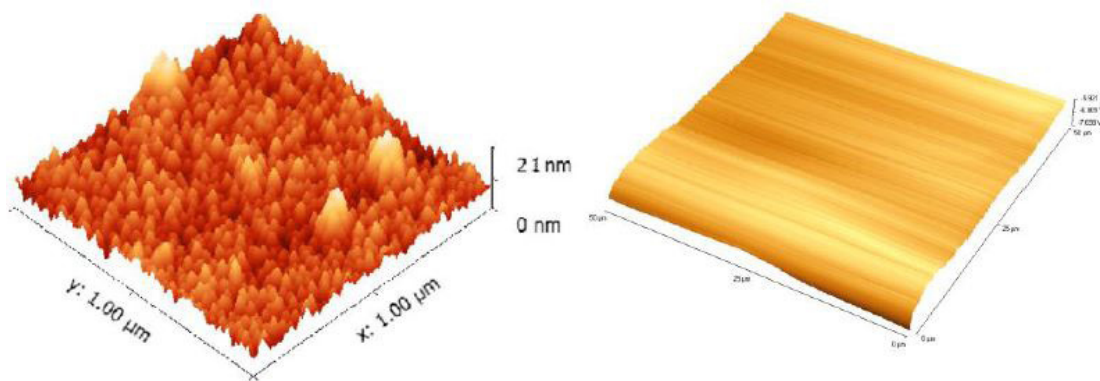


Fig. 5. UV-Vis spectra analysis of (i) Z and (ii)  $Z_A$  (iii)  $Z_B$  (iv)  $Z_C$  (v)  $Z_D$



The photo-degradation reaction can be schematically represented as follows<sup>24</sup>

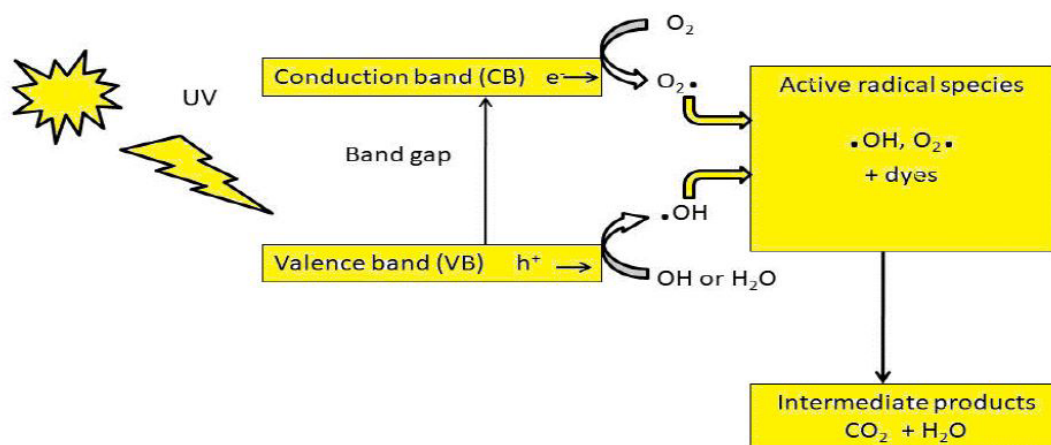


Fig. 6. AFM images of SEM analysis of (i) Z and (ii) Z<sub>B</sub>

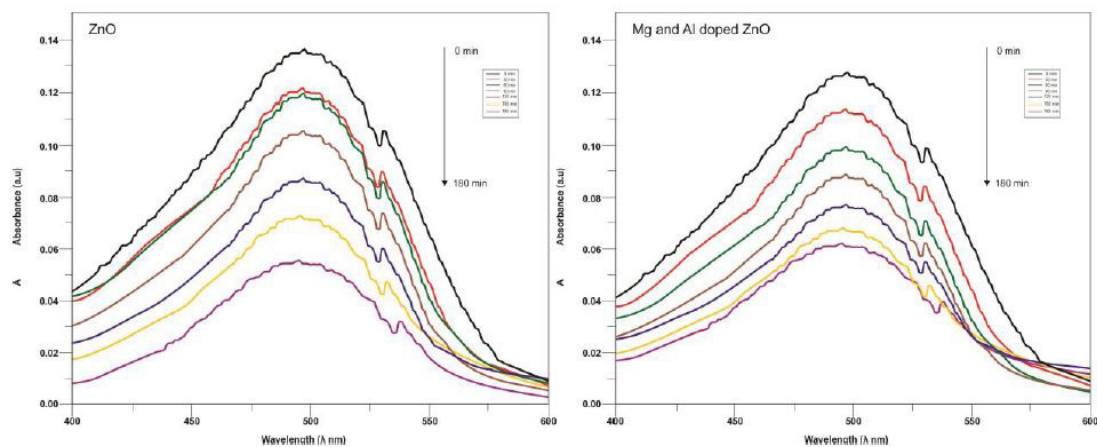


Fig. 7. Absorbance spectra of (i) Z and (ii) Z<sub>B</sub>

The photodegradation efficiency of nanomaterials was calculated by following formula<sup>25</sup>,

$$D (\%) = (A_0 - A_t) / (A_0) \times 100 \quad (3)$$

Where, D is the degradation efficiency (in %).  $A_0$  is the UV absorption of dye with sun light irradiation time (0 min) and  $A_t$  is the UV absorption of dye after UV-light irradiation (t-min).

Figure 7 (i) and (ii) shows the UV-Vis absorption spectra of congedred dye solution in the presence of Un-doped ZnO and Mg, Al doped ZnO nanocomposites with UV irradiation in different time intervals (30, 60, 90, 120, 150 and 180 mins). The photo-degradation efficiency calculated using equation (3) and the values were 55% for Un-doped ZnO and 83.6% for Mg and Al co-doped ZnO nanoparticles. The result of Photodegradation analysis of congo red dye with Un-doped and doped ZnO photocatalyst clearly presented a higher dye removal efficiency of the Mg and Alco-doped ZnO nanoparticles. Therefore, the experimental results concluded that the Mg and Alco-doped ZnO nanoparticles was a respectable dye removal catalyst compared to Un-doped ZnO nanoparticles. This route could be suitable for sewage and industrial water treatment.

### Conclusion

Un-doped ZnO and Mg, Al co-doped ZnO nanoparticles were prepared successfully using soft chemical method at room temperature. The synthesized samples were carefully characterized with XRD, FTIR, SEM-EDX, UV-Visible Spectroscopy and AFM and investigated different properties such as structural, morphological and optical. The hexagonal wurtzite structure of Un-doped ZnO and Mg, Al co-doped ZnO nanoparticles were confirmed by XRD analysis. SEM images exhibited the formation of nanoparticles and surface agglomeration. EDAX analysis results clearly indicated the percentage presence of material and its purity. AFM study indicated the surface morphology and average particle size of nanoparticles. The photo-degradation efficiency of Mg and Al co-doped ZnO (83.6%) nanoparticles owed superior performance than un-doped ZnO (55%) nanoparticles against congo red dye solution under UV irradiation. Ultimately, prepared nanoparticles will show a promising effect in waste water treatment for many industries.

### References

1. Forgacs, E., T. Cserháti, and G. Oros, Removal of synthetic dyes from wastewaters: a review. *Environment International*, **30** (7): p. 953-971 (2004)
2. Namasivayam, C. and D.J.S.E. Arasi, Removal of congo red from wastewater by adsorption onto waste red mud. *Chemosphere*, **34** (2): p. 401-417 (1997).
3. Chen, D., et al., Efficient removal of dyes by a novel magnetic Fe<sub>3</sub>O<sub>4</sub>/ZnCr-layered double hydroxide adsorbent from heavy metal wastewater. *Journal of Hazardous Materials*, **243**: p. 152-160 (2012).
4. Malik, P.K. and S.K. Sanyal, Kinetics of decolourisation of azo dyes in wastewater by UV/H<sub>2</sub>O<sub>2</sub> process. *Separation and Purification Technology*, **36** (3): p. 167-175 (2004).
5. Fu, Y. and T. Viraraghavan, Fungal decolorization of dye wastewaters: a review. *Bioresource Technology*, **79** (3): p. 251-262 (2001).
6. Mittal, A., et al., Adsorptive removal of hazardous anionic dye "Congo red" from wastewater using waste materials and recovery by desorption. *Journal of Colloid and Interface Science*, **340** (1): p. 16-26 (2009).
7. Walker, G.M. and L.R. Weatherley, Adsorption of acid dyes on to granular activated carbon in fixed beds. *Water Research*, 1997. **31**(8): p. 2093-2101.
8. Acemioğlu, B., Adsorption of Congo red from aqueous solution onto calcium-rich fly ash. *Journal of Colloid and Interface Science*, **274** (2): p. 371-379 (2004).
9. Qiu, R., et al., Photocatalytic activity of polymer-modified ZnO under visible light irradiation. *Journal of Hazardous Materials*, **156** (1-3): p. 80-85 (2008).
10. Devipriya, S. and Yesodharan, S. "Photocatalytic degradation of pesticide contaminants in water," *Solar Energy Materials and Solar Cells*, vol.86, No.3, pp. 309-348 (2005).

11. Muthukumar, S. and Gopalakrishnan, R., Structural, FTIR and photoluminescence studies of Cu doped ZnO nanopowders by co-precipitation method. *Optical Materials*, **34** (11), pp.1946-1953 (2012).
12. Shinde, V.R., Gujar, T.P., Lokhande, C.D., Mane, R.S. and Han, S.H., Mn doped and undoped ZnO films: A comparative structural, optical and electrical properties study. *Materials Chemistry and Physics*, **96** (2-3), pp.326-330 (2006).
13. Kumar, S.S., Venkateswarlu, P., Rao, V.R. and Rao, G.N., Synthesis, characterization and optical properties of zinc oxide nanoparticles. *International Nano Letters*, **3** (1), p.30 (2013).
14. Wu, Fei, Engineering and Applied Science Theses & Dissertations. *IJEA*, 141(2015).
15. Raja, K., Ramesh, P.S. and Geetha, D., Synthesis, structural and optical properties of ZnO and Ni-doped ZnO hexagonal nanorods by Co-precipitation method. *Spectrochimica Acta Part A: Molecular and Biomolecular Spectroscopy*, **120**, pp.19-24 (2014).
16. Sajid Husain, F. Rahman, Nasir Ali, Dr. Parvez Ahmad Alvi, *Optoelectron*, 28-32,
17. Bhatia, S., Verma, N. and Bedi, R.K., Optical application of Er-doped ZnO nanoparticles for photodegradation of direct red-31 dye. *Optical Materials*, **62**, pp.392-398 (2016).
18. Kumar, M., Singh, B., Yadav, P., Bhatt, V., Kumar, M., Singh, K., Abhyankar, A.C., Kumar, A. and Yun, J.H., Effect of structural defects, surface roughness on sensing properties of Al doped ZnO thin films deposited by chemical spray pyrolysis technique. *Ceramics International*, **43** (4), pp.3562-3568 (2017).
19. Qiu, X., Li, G., Sun, X., Li, L. and Fu, X., Doping effects of Co<sup>2+</sup> ions on ZnO nanorods and their photocatalytic properties. *Nanotechnology*, **19**(21), p.215703 (2008).
20. Piranavan Kumaravadivel, Grace A. Pan, Yu Zhou, Yujun Xie, Pengzi Liu, Judy J. Cha, *APL Materials*, **5** (2017).
21. Majumder, S.B., Jain, M., Dobal, P.S. and Katiyar, R.S., Investigations on solution derived aluminium doped zinc oxide thin films. *Materials Science and Engineering: B*, **103** (1), pp.16-25 (2003).
22. Bechambi, O., Touati, A., Sayadi, S. and Najjar, W., 2015. Effect of cerium doping on the textural, structural and optical properties of zinc oxide: role of cerium and hydrogen peroxide to enhance the photocatalytic degradation of endocrine disrupting compounds. *Materials Science in Semiconductor Processing*, **39**, pp. 807-816.
23. N.P. Radhika Rosilda Selvin Rita Kakkar Ahmad Umar, *Journal of Nanoscience and Nanotechnology* (2016).
24. Mehrabian, M. and Esteki, Z., Degradation of methylene blue by photocatalysis of copper assisted ZnS nanoparticle thin films. *Optik*, **130**, pp.1168-1172 (2017).
25. Ilyas, H., Qazi, I.A., Asgar, W. and Awan, M.A., Photocatalytic degradation of nitro and chlorophenols using doped and undoped titanium dioxide nanoparticles. *Journal of Nanomaterials*, p.21(2011).